

Tunable optical source for the interrogation of Bragg gratings via spectral scanning

A. S. Paterno, J. L. Fabris and H. J. Kalinowski
CEFET-PR — 80230-901 Curitiba, Brazil

ABSTRACT

This paper describes the implementation of an interrogation system with a tunable Erbium doped fiber ring-laser (EDFL). The EDFL is used to illuminate optical devices like Bragg gratings, so that it can also be used as an interrogation system to determine the spectral characteristics of the devices. An intra-cavity Fabry-Perot filter, driven by a dedicated voltage ramp generator, tunes the EDF laser. The resulting optical signal is captured by a photodetector and analyzed in a personal computer. The apparatus can be used as an optical spectrum analyzer for passive components and as an interrogation system for multiplexed fiber Bragg grating based sensors. As an application example, the temperature inside a concrete beam submitted to systematic heating and vibrations has been remotely measured with the system.

Keywords: Fiber laser, interrogation technique, Bragg grating sensor, identification system

1. INTRODUCTION

When acting as a sensor, Fiber Bragg Gratings (FBG) must be illuminated in a way that one can monitor the center wavelength of the light it reflects. The FBG will reflect a limited band of the spectrum of the incident light as it is scattered by each plane that forms the grating. The refractive index modulation forming the grating along the fiber causes the incident light to be progressively out of phase and the fraction of it that is not coincident with the resonance wavelength will be canceled out. The contributions of the scattered light from each grating plane add constructively if the light satisfies the Bragg condition, forming a back reflected peak, centered on a wavelength that is determined by the physical parameters of the FBG.¹ Since the response of the FBG sensor will depend on these parameters, mechanical or thermal perturbations will alter the spectral characteristics of the signal that propagates through it. In order to investigate such perturbations, one usually uses an optical source with a broad spectrum to illuminate the device. This spectrum is sufficiently broad to illuminate the whole spectrum of operation of the FBG, which in our case is the optical C-band.

Another way to demodulate the center wavelength of the back-reflected light and detect its variations caused by perturbations is to illuminate the FBG with a scanning frequency light so that its wavelength covers the whole band of the spectrum on which the fiber sensor operates. This can be done with tunable optical filters or sources with a bandwidth narrower than that of the FBG.

Several approaches can be found in the literature using Fabry-Perot (FPF), acousto-optic (AOTF) and other filters, or even with tunable FBG.² With such identification systems one obtains several convolutions of the transfer function of the filter, which can be dynamically tuned at different wavelengths, with the FBG reflection spectrum. The resolution of the system will depend basically on filter and sensor bandwidths, as well as on the reflected power of the signal. A tunable semiconductor laser could also be used equivalently as the interrogating mean as described in literature.³

In this paper an identification system is reported in which a tunable EDF ring laser was used, in place of a scheme consisting of a wideband source followed by a tunable filter, for the purpose of illuminating the fiber Bragg grating sensors and evaluating their behavior under operating conditions or when the spectrum profile of the device is unknown.

Corresponding author: A.S.Paterno, Centro Federal de Educação Tecnológica do Paraná, Av. Sete de Setembro, 3165 — 80230-901 Curitiba, Brazil, phone: +55 41 310 4703.
E-mail: sade@cpgei.cefetpr.br (A.S.Paterno)

2. THEORETICAL CONSIDERATIONS

In an identification system with a tunable filter or laser as described, the reflected energy from an FBG, E_R , in one scanning period, is²:

$$E_R = \frac{RI\Delta\lambda_{BGS}}{f} \quad (1)$$

where R is the reflectivity of the grating, $\Delta\lambda_{BGS}$ is its bandwidth, I is the intensity of the source, and f is the scanning rate. With a tunable filter, the available energy to detection, E_D , is:

$$E_D = \frac{E_R\Delta\lambda_f}{\lambda_i} \quad (2)$$

where $\Delta\lambda_f$ is the filter bandwidth and λ_i the wavelength scanning range. If one supposes $\Delta\lambda_f \approx 1\%\lambda_i$, the available energy for detection per scan for a reflectivity $R = 100\%$ will be only $1\%E_R$. It means that if one needs high resolution, particularly if high reflectivity gratings are not available, optical sources with higher power and spectral density are preferable rather than ASE sources, lamps or any other lower power sources.

3. SYSTEM DESCRIPTION

The fundamental device of the identification system is an electronically tunable Erbium-doped fiber ring laser with an intra-cavity Fabry-Perot filter (FPF) whose schematic design is presented on fig.1(a). The EDF has 17 m with Er concentration of 280 ppm and cutoff wavelength of less than 1480 nm, allowing only the fundamental mode LP_{01} at the pump wavelength 1480 nm. The pump power of approximately 70 mW is introduced inside the EDF through a WDM coupler, which is part of an IFAM(Integrated Fiber Amplifier Module) used in the laser. The optical isolator, also integrated with the WDM coupler, prevents bi-directional propagation in the cavity. The laser light propagates in the clockwise direction. Through the output coupler, approximately 80% of the laser light is emitted and the other 20% are used for optical feedback. The original configuration of the EDFL consisted of two intra-cavity filters which optimized the linewidth of the output light.⁴ In order to automatize the tunability of the EDFL, the mechanical filter was removed. Power and linewidth optimization deteriorated, but the electronic tuning of the remaining FPF in the cavity made the automatization possible.⁵ The tuning range of the FPF can be set by means of a voltage applied to its terminals which are connected to the PZT that moves the mirrors of the filter. Setting the voltage from 3.35 V to 8.75 V, the laser can be tuned from 1525 to 1565 nm at the room temperature of 24°C. Between these wavelengths the intensity of the laser output is approximately constant and higher than -20 dBm and its linewidth is also constant with an estimated value of 67 pm, as can be seen on fig. 1(b). An electronic circuit that generates a triangular voltage is applied to the terminals of the Fabry-Perot filter. It tunes the wavelength of the laser periodically along the C-band in a frequency of 25 Hz. The switching frequency is limited by the fact that the lifetime of the EDF ${}^4I_{13/2}$ level is around 10 ms.⁶ It would be theoretically possible to switch between different wavelengths on the EDFL with a maximum frequency of 1/10 ms, which is the inverse of the excited level lifetime in the EDF.

3.1. The complete system

The complete configuration of the system is shown in fig. 2(a). The beam from the laser is splitted at port 1 by the 3dB coupler and illuminates equally the FBG1 and FBG2, and the Bragg grating sensor (BGS) to be monitored. The signals reflected by these three FBG are combined at port 2 in the coupler and acquired by a photodetector circuit connected to a digital oscilloscope. The data generated on the oscilloscope are transferred via RS-232 interface to a personal computer where they will be processed. FBG1 and FBG2 are kept at constant temperature by means of a Peltier on which they are thermally coupled and serve also as references in the acquired spectrum. The BGS has a center wavelength of 1539 nm; FBG1 and FBG2 are centered respectively on 1529.19 nm and 1534.39 nm. All the FBG have more than 90% reflectivity and were imprinted at the Fotorefractive Devices Unit in CEFET-PR,⁷ using a phase mask illuminated interferometer operating at the wavelength of 266 nm.⁸

The response obtained by the oscilloscope and acquired by the computer shows the signal proportional to the output power as a function of the instant at which it is acquired, that is, as a function of the wavelength at

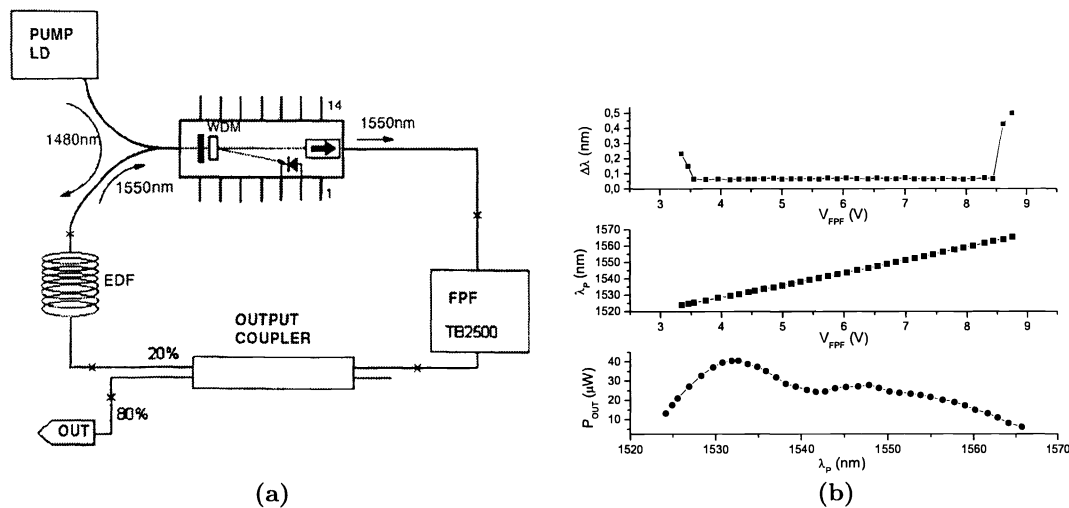


Figure 1. EDFL configuration (a); Linewidth vs FPF voltage (top); center wavelength vs FPF voltage (center); EDFL output power vs center wavelength (bottom)(b).

which the EDFL is tuned at the moment. In order to convert the time scale of this data into the wavelength's, two previously known stable points on the acquired spectrum are provided by FBG1 and FBG2 reflection peaks. Since there are constant references in the spectrum, it is unnecessary to compensate any temperature perturbation in the devices, namely the FPF and the EDF coil, which compose the EDFL and could affect the spectrum. Temperature variation in the EDFL can affect its gain and tuning, but not the position of the reference peaks provided by FBG1 and FBG2. The linear correspondence between the instants of acquisition and wavelengths is guaranteed by the linear response of the FPF with voltage. Let λ_{B1} and λ_{B2} be the reflection peaks of FBG1 and FBG2, t_1 and t_2 the instants at which they are acquired. By means of a linear equation it is possible to obtain the relation between such time of acquisition and wavelength:

$$\lambda = (t - t_2) \left(\frac{\lambda_{B2} - \lambda_{B1}}{t_2 - t_1} \right) + \lambda_{B2} \quad (3)$$

This process is repeated at the scanning rate of the voltage applied at the FPF 25 Hz. This rate determines the maximum frequency that could be detected by the BGS. On fig. 2(b) one scan can be seen as a photograph of the oscilloscope screen.

4. EXPERIMENTAL APPLICATION

In order to demonstrate remote measurements of temperature taken by the system, the BGS is installed inside a concrete beam and is submitted to intense heat for 75 minutes. During this period, the thermal perturbation inside the beam is measured via BGS and another independent FBG sensor. Both had their reflection spectra simultaneously monitored during the time the beam is submitted to the heat. Acquisitions are made periodically in intervals of approximately 3 minutes. The measuring and control systems and the laser are installed in another laboratory, 50 m far away from the concrete beam. The independent sensor is illuminated by a superluminescent diode and is monitored by an optical spectrum analyzer. In fig. 3 one can see that the BGS is connected to the EDFL by means of a 50 m long optical cable to the port 4 of a 3 dB coupler. The references FBG1 and FBG2 are also connected to the coupler output port. The references and the BGS are illuminated by the EDFL and the light reflected by them is recombined in the coupler and collected by a photodetector being constantly monitored by a digital oscilloscope. In order to process data after acquisition, the calibration equation of the

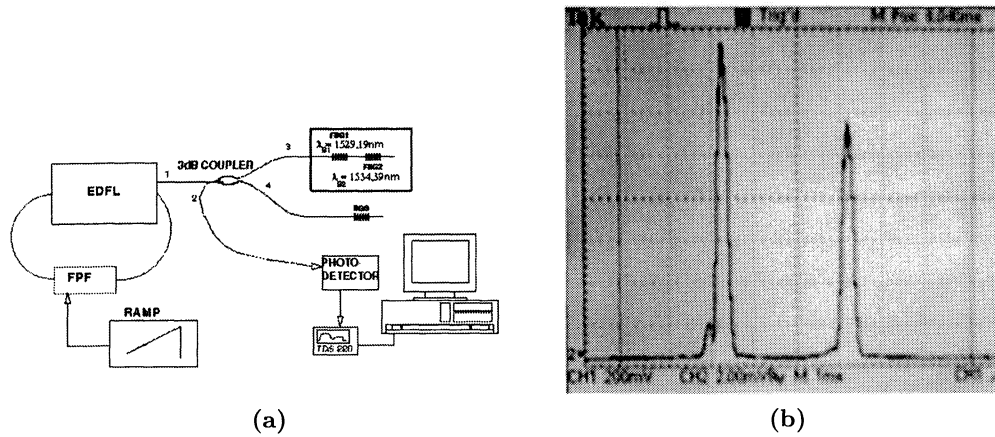


Figure 2. Diagram of the first setup using the EDFL for the interrogation of the BGS. Sensors inside the black-box are thermally stabilized by a Peltier device (a); Acquired spectrum of the reflected signal from the two reference gratings FBG1 and FBG2 (b).

BGS is previously obtained with an OSA and it is represented by:

$$\lambda_{BGS} = 1543.73 + 0.00997T \quad (4)$$

where λ_{BGS} is the center wavelength of the sensor in nanometer and T is the temperature in degree Celsius. The reference gratings in this case had constant wavelengths $\lambda_{B1} = 1529.12$ nm for FBG1 and $\lambda_{B2} = 1534.28$ nm for FBG2. Temperature in the laboratory with the EDFL was stable, therefore the Peltier device was not used to stabilize the temperature of FBG1 and FBG2.

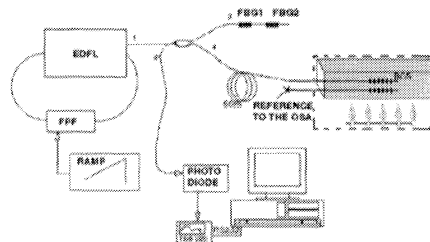


Figure 3. Diagram of the system to measure temperature inside a concrete beam located 50 m away from the measuring apparatus.

5. RESULTS

On fig. 4(a) the data from four spectra can be seen. They are already converted to the wavelength scale and illustrate the variations occurring during the perturbation in the BGS. The four peaks corresponding to the highest wavelengths are associated to the monitored BGS. The first peak around 1543.54 nm corresponds to one of the first measurements made without temperature perturbation. As the temperature increases, this peak moves to the right in the spectrum. The last acquisition shown corresponds to the reflection peak of the BGS around 1545.52 nm. Each spectrum is obtained after the oscilloscope calculates the mean spectrum from 128 samples. Each sample is the set of points obtained with the acquisition from one scan of the ramp generator.

Using the peak values associated to λ_{BGS} and the equation (4), it is possible to calculate the temperatures of the BGS. The calculated values are compared to the values measured by the independent sensor. The

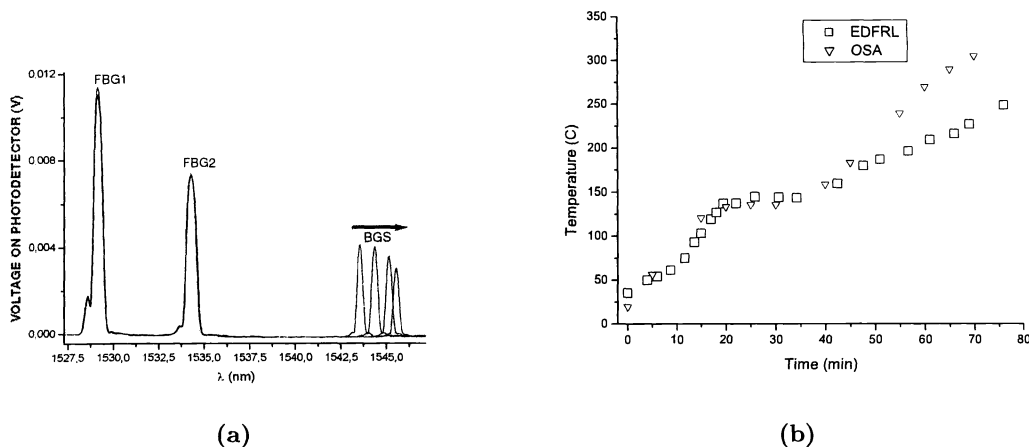


Figure 4. Evolution of the reflection spectrum from a BGS with systematic increase in temperature (a); comparison between measurements of temperature made with the reference system utilizing an OSA and with the EDFL system (b).

comparison can be seen on fig. 4(b), which shows the temperatures obtained with both systems. Since they were independent and located in different laboratories, the points shown on the plot are acquired at different rates.

With the independent sensor, a series of temperatures were obtained varying from 19.8°C up to 304.4°C after 70 minutes of systematic heating. With the EDFL system, temperature varied from 35.4°C up to 226.6°C after 70 minutes, as can be observed on fig. 4(b).

Considering the isolated spectra, each one is made by a set of 2500 points per scan along the 40 nm EDFL range, the resolution can then be determined: $40 \text{ nm}/2500 = 16 \text{ pm}$, showing that 5 points are necessary to resolve a bandwidth of 0.08 nm of an FBG. This bandwidth can be considered standard in FBG sensors. The estimated uncertainty was 0.125 nm.

6. DISCUSSION

In fig. 4(a), it was assumed that the references FBG1 and FBG2 were kept stable at $\lambda_{B1} = 1529,12 \text{ nm}$ and $\lambda_{B2} = 1534,28 \text{ nm}$. The differences between the amplitudes in the spectrum of FBG1 and FBG2 is due to the non-uniform profile of the EDFL gain spectrum (see output power vs. center wavelength on fig. 1(b)), having its peak around the region of FBG1. With the increase in temperature, the reflectivity of the BGS sensor changed, showing a decrease that can be seen in fig. 4(a) in the region of 1543 nm.

The region in fig. 4(b) showing a constant slope around 20 minutes, occurred because of a decrease in the gas pressure in the heating process. More pressure was subsequently provided to continue increasing the temperature.

During the first 45 minutes of heating, as can be seen in fig. 4(b), the measured temperature of both systems follow one another. From this fact one can infer that until this moment the measurements are relatively reliable. Beyond this point, there is a divergence between data acquired from the OSA system and the EDFL system. This has happened probably because the two sensors were affected by hard vibrations on the beam, which was also being characterized under vibrational aspects related to its resonance frequency behavior after increase in temperature and vibration of the concrete*. It is probable that macroscopic cracks could have happened inside

*This beam was being used in an experiment intended to determine the resonance frequency of the concrete with FBG accelerometers when temperature increased. For this purpose, vibrations were induced on the beam with a hammer.

the beam in the region where the sensors were installed. With air inside the cracks, a gradient of temperature could have affected the acquired values. The change in temperature and the effect of mechanical vibrations in beam might have caused a mechanical perturbation in the sensor, disturbing the center wavelength reflected by the sensor.⁹ During the first 45 minutes, the mean difference between measurements with the EDFL and the independent sensor was 12,8°C with 18,2°C of deviation. After that, the mean difference increased to 50,7°C with deviation 32°C.

Concerning the performance of the EDFL system, the evolution of the spectra can be obtained almost instantaneously, based on the fact that the limitation is on the acquisition electronics, allowing an interrogation performance under this standpoint equivalent to the optical spectrum analysers with discrete diffraction gratings with which one can obtain a wavelength scan rate of 1 nm/ms, just like the EDFL in the C-band covering 40 nm in 1/25 s.

7. CONCLUSIONS

The developed system performs and executes several functions of an optical spectrum analyzer, such as the determination of spectral response of passive devices; it can be used with interrogation techniques, because the intra-cavity FPF can easily modulate the EDFL signal in the whole C-band, not limited by a narrow tuning band. In this case, it can be used dynamically to evaluate the behavior of distributed sensors. It has to be stressed that although the relatively low output power of this EDFL, its high spectral density allows the direct acquisition of FBG spectra with low reflectivity, which could not be observed using a superluminescent LED followed by a scanning filter.

ACKNOWLEDGMENTS

The authors would like to thank the Agência Nacional do Petróleo (ANP) and the Financiadora de Estudos e Projetos (FINEP) for the financial support by means of the Human Resources Program of the ANP in the Gas and Oil Sector (PRH-ANP/MCT - PRH10 - CEFET-PR); the CAPES, CNPq and LITS/TECPAR for the support to the laboratory. Authors would also like to thank Dr. Elisabeth Penner (DACOC/CEFET-PR), J. C. C. da Silva, C. Martelli and R. Falate for the experimental support.

REFERENCES

1. R. Kashyap, *Fiber Bragg Gratings*, Academic Press, London, UK, 1999.
2. A. D. Kersey, M. A. Davis, H. J. Patrick, M. LeBlanc, K. P. Koo, C. G. Askins, M. A. Putnam, and E. J. Friebele, "Fiber grating sensors," *Journal of Lightwave Technology* **15**(8), pp. 1442–1463, 1997.
3. T. Coroy, L. Chappell, N. Guillermo, S. Huang, and R. Measures, "Peak detection demodulation of a Bragg fiber optic sensor using a gain-coupled distributed feedback tunable laser," *12th International Conference on Optical Fiber Sensors* **16**, pp. 210–212, 1997.
4. M. J. Pontes, M. J. D. dos Santos, I. Abe, H. J. Kalinowski, and M. T. M. R. Giralardi, "Analysis of longitudinal mode suppression in a fiber ring laser containing two optical filters," *Fiber and Integrated Optics* **1**(19), pp. 57–65, 2000.
5. A. S. Paterno, "Laser sintonizável para caracterização de dispositivos óticos," Master's thesis, CEFET-PR, Curitiba, Brasil, October 2003.
6. Y. T. Chieng, G. J. Cowle, and R. A. Minasian, "Optimization of wavelength tuning of Erbium-doped fiber ring lasers," *Journal of Lightwave Technology* **14**(7), pp. 1730–1738, 1996.
7. J. C. C. da Silva, J. L. Fabris, R. C. Chaves, I. Abe, H. J. Kalinowski, J. L. Pinto, and C. L. Barbosa, "Development of Bragg grating sensors at CEFET-PR," *Optics and Lasers in Engineering* **5-6**(39), pp. 511–523, 2003.
8. J. C. C. da Silva, R. Falate, J. L. Fabris, H. J. Kalinowski, J. L. Pinto, and R. N. Nogueira, "Production of fiber Bragg gratings in phase mask interferometers," *ConfTele: Proc. 4th. Conference on Telecommunications - Aveiro, Portugal*, pp. 449–451, 2003.
9. A. Othonos and K. Kalli, *Fiber Bragg Gratings: Fundamentals and Applications in Telecommunications and Sensing*, Artech House, Boston, 1999.